UNIVERSITYOF
BIRMINGHAM

A simple mechanism for integration of quorum sensing and cAMP signalling in V. cholerae

Walker, Lucas; Haycocks, James; van Kessel, Julia C.; Dalia, Triana N; Dalia, Ankur B; Grainger, David

[Link to publication on Research at Birmingham portal](#)

Chromosomes and Gene Expression, Microbiology and Infectious Disease

A simple mechanism for integration of quorum sensing and cAMP signalling in *V. cholerae*

Lucas M. Walker, James R.J. Haycocks, Julia C. van Kessel, Triana N. Dalia, Ankur B. Dalia, David C. Grainger

School of Biosciences, University of Birmingham, Edgbaston B15 2TT , UK • Department of Biology, Indiana University, Bloomington, Indiana , USA

Abstract

Many bacteria use quorum sensing to control changes in lifestyle. The process is regulated by microbially derived "autoinducer" signalling molecules, that accumulate in the local environment. Individual cells sense autoinducer abundance, to infer population density, and alter their behaviour accordingly. In *Vibrio cholerae*, quorum sensing signals are transduced by phosphorelay to the transcription factor LuxO. Unphosphorylated LuxO permits expression of HapR, which alters global gene expression patterns. In this work, we have mapped the genome-wide distribution of LuxO and HapR in *V. cholerae*. Whilst LuxO has a small regulon, HapR targets 32 loci. Many HapR targets coincide with sites for the cAMP receptor protein (CRP) that regulates the transcriptional response to carbon starvation. This overlap, also evident in other *Vibrio* species, results from similarities in the DNA sequence bound by each factor. At shared sites, HapR and CRP simultaneously contact the double helix and binding is stabilised by direct interaction of the two factors. Importantly, this involves a CRP surface that usually contacts RNA polymerase to stimulate transcription. As a result, HapR can block transcription activation by CRP. Thus, by interacting at shared sites, HapR and CRP integrate information from quorum sensing and cAMP signalling to control gene expression.

eLife assessment

This paper provides **valuable** new information on the mechanisms by which Vibrio cholerae integrates and responds to environmental signals. While the strength of the evidence provided in the paper in support of the conclusions made and the model proposed is **solid**, there are several issues that if addressed will strengthen the study further. The work is relevant for a broad audience of microbiologists interested in the mechanisms by which bacteria sense their environment.

Introduction

Vibrio cholerae is a Gram-negative bacterium responsible for the human disease cholera[1]. Estimates suggest 3 million annual infections, of which 100 thousand are fatal[2]. Most disease instances are attributed to the El Tor *V. cholerae* biotype, which is responsible for the ongoing 7th cholera pandemic[3]. Globally, over 1 billion people inhabit areas of endemicity and future climatic change is likely to exacerbate the risk of illness[2],[4]. The success of *V. cholerae* as a pathogen is underpinned by an ability to colonise both aquatic ecosystems and the human intestinal tract[1]. In waterways, *V. cholerae* prospers by forming biofilms on arthropod exoskeletons. Degradation of these chitinous surfaces ultimately liberates *N*-acetylglucosamine (GlcNAc) for metabolism by the microbe[5]. Upon ingestion by a human host, *V. cholerae* express genetic determinants for acid tolerance, intestinal colonisation, and virulence. Diverse transcription factors regulate the transition and respond to signals including bile[6], temperature[7], nucleotide second messengers[8],[9], and chitin availability[5]. Understanding these regulatory networks is important to determine how *V. cholerae* can switch between environments to cause disease outbreaks[3],[10],[11].

Quorum sensing is key for the transition of *V. cholerae* between ecological niches[12]. Briefly, *V. cholerae* produce at least 3 autoinducer (AI) signalling molecules: cholera AI-1 (CAI-1), AI-2, and 3,5-dimethylpyrazin-2-ol (DPO)[13]. In the environment, these compounds are detected by receptors in neighbouring cells and indicate population density. Importantly, whilst AI-2 and DPO are produced by multiple bacterial species, CAI-1 is only made by other members of the *Vibrio* genus[14]. Thus, *V. cholerae* can determine the crude composition of bacterial populations. In the absence of their cognate AIs, when population density is low, the receptors for CAI-I and AI-2 target the transcription factor LuxO for phosphorylation via a phosphorelay system[13],[15],[16]. When phosphorylated, LuxO upregulates the production of four small quorum regulatory RNAs (Qrrs)[17]. In turn, the Qrrs control expression of two global transcription factors: AphA and HapR[17]–[19]. Importantly, whilst AphA production is activated by Qrrs, synthesis of HapR is repressed. Hence, AphA and HapR control gene expression at low and high cell density respectively[13],[19]. A simplified outline of the LuxO dependent regulatory pathway for HapR is illustrated in Figure 1a.
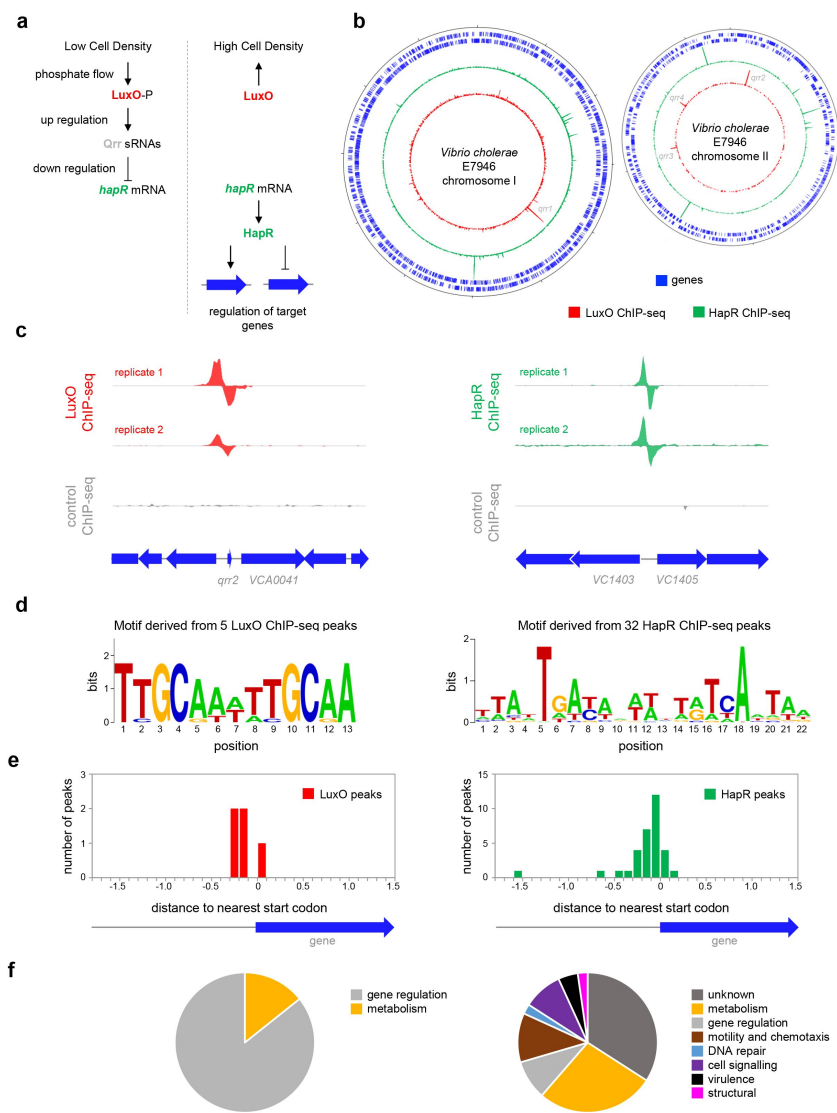
Figure 1:

Genome-wide distribution of HapR and LuxO in *Vibrio cholerae*.

a. Simplified schematic overview of quorum sensing in *Vibrio cholerae*. At low cell density, expression of HapR is repressed by the Qrr sRNAs that depend on phosphorylated LuxO for activation of their transcription. Arrows indicate activation and bar ended lines indicate repression. For clarity, not all protein factors involved in the cascade have been included.

b. Binding of LuxO and HapR across both *Vibrio cholerae* chromosomes. In each plot the outer two tracks (blue) are genes orientated in the forward or reverse direction. The LuxO and HapR ChIP-seq binding signals are shown in red and green. LuxO binding peaks corresponding to the *qrr1-4* loci are indicated. Tick marks are 0.25 Mbp apart.

c. Example LuxO and HapR ChIP-seq binding peaks. ChIP-seq coverage plots are shown for individual experimental replicates. Data for LuxO and HapR are in green and red respectively. Signals above or below the horizontal line correspond to reads mapping to the top or bottom strand respectively. Gene are show as block arrows.

d. Sequence motifs derived from LuxO and HapR binding peaks using MEME.

e. Positions of LuxO and HapR binding peaks with respect to genes. The histograms show the distribution of binding peak centres with respect to the start codon of the nearest gene.

f. Pie charts showing gene classes targeted by LuxO and HapR.

Identified as a regulator of *hapA*, required for *V. cholerae* migration through intestinal mucosa, HapR is a TetR-family member that binds DNA as a homodimer via a N-terminal helix-turn-helix motif[20],[21]. Many clinical isolates of pandemic *V. cholerae* have lost the ability to properly express HapR and this may indicate adaptation to a more pathogenic lifestyle[3],[10],[22]. In *V. cholerae*, HapR regulates the expression of ~100 genes to promote 'group behaviours' including natural competence, repression of virulence genes, and escape from the host intestinal mucosa[23]. In other *Vibrio* spp., equivalent regulons are larger. For example, LuxR in *Vibrio harveyi* regulates over 600 genes[24]. Expression of HapR can be influenced by other factors. In particular, cAMP receptor protein (CRP), a regulator that controls metabolism of alternative carbon sources, including chitin, upregulates HapR[25]. In this study, we used chromatin immunoprecipitation and DNA sequencing (ChIP-seq) to

identify direct DNA binding targets of HapR and its upstream regulator, LuxO. We show that the degenerate DNA consensus bound by HapR frequently overlaps targets for CRP. At such sites, HapR and CRP co-operatively bind offset faces of the double helix. Strikingly, this occludes a key CRP surface required to activate transcription. This simple mechanism allows *V. cholerae* species to integrate quorum sensing, and cAMP signalling, in the control of gene expression.

Results

Genome-wide DNA binding by HapR and LuxO in Vibrio cholerae

Whilst the impact of HapR on global gene expression in *V. cholerae* has been investigated, it is not known which HapR responsive genes are directly controlled by the protein[23]. Similarly, the extent of the direct LuxO regulon is unknown. Hence, we sought to map the binding of LuxO and HapR across the *V. cholerae* genome. To facilitate this, *luxO* and *hapR* were cloned in plasmids pAMCF an pAMNF respectively. The resulting constructs, encoding LuxO-3xFLAG or 3xFLAG-HapR, were used to transform *V. cholerae* strain E7946. In subsequent ChIP-seq experiments, anti-FLAG antibodies were used to select fragments of the *V. cholerae* genome bound with either LuxO or HapR. The derived binding profiles are shown in Figure 1b. In each plot, genes are shown as blue lines (outer two tracks) whilst the LuxO and HapR binding signals are red and green respectively (inner two tracks). Examples of individual binding peaks for each factor are shown in Figure 1c. In total, we identified 5 and 32 peaks for LuxO and HapR binding respectively (Table 1). Previous work identified targets for LuxO adjacent to genes encoding the 4 Qrr sRNAs. We recovered all of these known LuxO targets, and an additional binding site was identified between *VC1142* and *VC1143*. These divergent genes encode cold shock-like protein CspD, and the Clp protease adaptor protein, ClpS, respectively. Note that the LuxO binding signal at this locus is small, compared to the *qrr*1-4 targets (Figure S1). To identify the sequence bound by LuxO, DNA regions overlapping LuxO binding peaks were inspected using MEME. The motif identified matches the known consensus for LuxO binding and was found at all LuxO targets (Table 1 and Figure 1d)[26]. The positions of LuxO binding sites with respect to genes, and the functions encoded by these genes, are summarised in Figures 1e and 1f respectively. Of the 32 peaks for HapR binding, 4 correspond to previously identified direct targets (*hapR*[27], *VC0241*[28], *VC1851*[29] and *VCA0148*[28]). Similarly, a DNA motif common to all HapR ChIP-seq peaks matched prior descriptions of the DNA target for HapR (Figure 1d). Occurrences of this HapR binging motif were most frequent in the 200 bp preceding a gene start codon (Figure 1e). Most often, the genes adjacent to HapR binding peaks encode protein functions related to metabolism, motility, and chemotaxis (Figure 1f). Overall, our data suggest that LuxO primarily regulates gene expression via the 4 Qrr sRNA molecules. Conversely, the genome-wide distribution of HapR is consistent with that of a global gene regulator with many undefined regulatory roles.

Locations of binding peaks from ChIP-seq experiments

peak centre	gene(s)[4]	site location	site sequence
	HapR ChIP-seq peaks		
	chromosome I		
99874	VC0102<(VC0103)	99863.5	aaattaataaaactgtcattta
213457	(VC0205)>VC0206	213452.5	taattgtgattcttatcaccaa
246366[1]	VC0240<>VC0241	246349.5	taattaagatggctataaacta
463584	VC0433		
514422	VC0484	514430.5	ctactgaccttttcatcaataa
516570	(VC0486)	516601.5	caactgagaaggcacacaatag
534714	(VC0502)	534691.5	ctattataagctctatcagtgt
547108	VC0515	547135.5	atagtaatattattgttaatag
613328[3]	VC0583[A]	613357.5	ttattgagtgggtacataacaa
716707	VC0668	716625.5	ctattgatgaggttatccacag
735309	VC0687<>VC0688		
882854	(VC0822)	882825.5	taattatccactttatcaattg
941187	VC0880	941164.5	cttttgacatttctgtcacaaa
978577	VC0916[R]	978540.5	taattaatatccagctcaatta
1356743	VC1280<>VC1281[A]	1356736.5	atattgatagaaataacaagtc
1379202	VC1298<>VC1299	1379180.5	ttcatgatagtttttgtaattat
1469384	VC1375<>VC1376	1469377.5	atattgatatatcacacatctt
1496023	VC1403[A]<(VC1404)>VC1405	1496025.5	tagttgatatttttataattgt
1533842	(VC1437)	1533854.5	tttgtgagtctcctgtcaataa
1990133[2]	VC1851	1990076.5	atattgagtaatcaattagtaa
2364721	(VC2212)	2364680.5	ctattaacagtttttatttataa
2509878	VC2352	2509882.5	ttagtgacagatgcgtcattaa
2667349	VC2486	2667368.5	taattattaatttgaacaatag
	chromosome II		
163808[1]	VCA0148	163810.5	taattgattattgtgtaactat
214589	(VCA0198)	214582.5	taattgataactttgacagtat
237008	VCA0218<>VCA0219[R]	237019.5	taaataatatgaatatcagtaa
247286	VCA0224<>VCA0225	247241.5	taaatgactaataagacaatta
598444	VCA0662<>VCA0663[R]	598403.5	tttgtaataaatttgtcattaa
630517	VCA0691[A,]	630559.5	ctattaacaggactgacattaa
862737	VCA0906		
910196	VCA0960[R]<>VCA0961	910181.5	ctgattataaatttgtaaatat
1021174	VCA1070	1021117.5	ctcctatccgattggtcactat
	LuxO ChIP-seq peaks		
	chromosome I		
1090129	qrr1<> VC1021	1090154	ttgcaaaatgcaa
1212442	VC1142<>VC1143	1212435	ttgcaaatcgcga
	chromosome II		
48415	qrr2	48347	ttgcaatttgcaa
772208	qrr3	772149	ttgcattttgcaa
908445	qrr4	908436	ttgcaatttgcaa

[1]Identified by Tsou and co-worlers[28]
[2]Identified by Waters and co-workers[29]
[3]Identified by Lin and co-workers[27]
[4]Identified as activated (A) or repressed (R) by Nielsen and co-workers[23]

HapR is a direct regulator of transcription at many target sites

We focused our attention on new HapR target promoters where adjacent coding sequence could be used to predict encoded protein function. For these 24 targets, regulatory DNA was cloned upstream of *lacZ* in plasmid pRW50T. Recombinants were then transferred to *V.*

cholerae E7946, or the Δ*hapR* derivative, by conjugation. Strains generated were cultured overnight before β-galactosidase activities were determined. The results are shown in Figure 2a. Promoters were categorised as inactive, unresponsive, repressed or activated by HapR. We identified 2 and 7 promoters subject to activation and repression by HapR respectively. Of the remaining promoters, 7 were inactive and 11 unresponsive to HapR in our conditions. Next, the 9 promoter DNA fragments responsive to HapR *in vivo* were cloned upstream of the λ*oop* terminator in plasmid pSR. The resulting constructs were then provided to housekeeping *V. cholerae* RNA polymerase, as templates for *in vitro* transcription, in the presence and absence of HapR. The results are shown in Figure 2b where the expected size of transcripts terminated by λ*oop* are marked with blue triangles[30]. Recall that the *VC1375* and *VC1403* promoters were activated by HapR *in vivo* (Figure 1a). Consistent with this, HapR also activated the *VC1375* promoter *in vitro* (Figure 3b, lanes 43-47). However, HapR did not activate *in vitro* transcription from the *VC1403* promoter (Figure 3b, lanes 48-53). Indeed, interpretation of these data were hampered because the location of the *VC1403* transcription start site (TSS) is not known[30]. Of the 7 promoters repressed by HapR *in vivo*, we observed repression in 6 cases *in vitro* (*hapR, VC0585, VC2352, VCA0219, VCA0663* and *VCA0960*) (lanes 7-42). Conversely, the *murQP* promoter (P*murQP*) subject to repression by HapR *in vivo*, generated no transcript *in vitro* (lanes 1-6).

Figure 2:

HapR is a direct repressor of transcription at many target promoters.

a. Activity of HapR targeted promoters in the presence and absence of HapR *in vivo*. The promoter regions of HapR targeted genes were fused to *lacZ* in plasmid pRW50T and constructs used to transform required bacterial strains. was measured in cell lysates taken from *Vibrio cholerae* E7946 (bars) or the Δ*hapR* derivative (open bars). containing the *VC0857* promoter cloned upstream of *lacZ* in pRW50T. Standard deviation is shown for three independent biological replicates. Cells were grown in LB medium. Promoters were classified as inactive if, in both the presence and absence of HapR, β-galactosidase activity was <2-fold higher than the equivalent no insert control.

b. Activity of HapR targeted promoters in the presence and absence of HapR *in vitro*. The gel images show results of *in vitro* transcription experiments. The DNA templates were plasmid pSR derivatives containing the indicated regulatory regions. Experiments were done with 0.4 µM RNA polymerase in the presence (0.25, 0.75, 1.0, 3.0, or 5.0 µM) and absence of HapR. Except for the *VC1375* promoter, where the maximum HapR concentration was 3.0 µM. The RNAI transcript is plasmid-derived and acts as an internal control. Expected transcript sizes, based on results from global transcription start site mapping experiments[30], are indicated. Note that no *VC1403* transcript was detected in this prior study[30].

Transcription from the murQP *promoter requires CRP* in vivo *and* in vitro

The *murQP* operon encodes functions important for recycling of peptidoglycan. Briefly, cell wall derived *N*-acetylmuramic acid (MurNAc) is transported across the inner membrane, and simultaneously phosphorylated, by the phosphotransferase system dependent permease MurP. Resulting MurNAc-6P is hydrolysed by MurQ to generate *N*-acetylglucosamine 6-phosphate (GlcNAc-6P). Intriguingly, GlcNAc-6P can also be derived from chitin break down and this coincides with expression of HapR. Hence, we focused on understanding the role of HapR bound upstream of *murPQ*. The HapR ChIP-seq binding signal at the *murQP* locus is

shown in Figure 3a and the associated regulatory region is shown in Figure 3b. The centre of the ChIP-seq peak for HapR is marked by an asterisk and the predicted binding site is highlighted green. We reasoned that our inability to detect transcription from P*murQP in vitro* was likely because an undefined transcriptional activator is absent (Figure 2b). Inspection of the DNA sequence upstream of *murQP* identified a close match to the consensus binding site for CRP (5'-TGTGA-N_6-TCACA-3'). Furthermore, this sequence was located 41.5 bp upstream, of the *murQP* TSS (Figure 3b). This is a common scenario for CRP dependent transcription activation[31]. To measure binding of CRP to the *murQP* regulatory region we used electrophoretic mobility shift assays (EMSAs). Consistent with our prediction, CRP bound to the *murQP* regulatory DNA (Figure 3c, lanes 1 and 2). To confirm that we had correctly identified the binding site for CRP we made a series of P*murQP* derivatives. The Δ183 and Δ211 DNA fragments have large upstream deletions (sites of truncation are shown by inverted triangles in Figure 3b, which mark the 5' end of the remaining promoter DNA) but still bind CRP (Figure 3c, lanes 3-6). Conversely, point mutations -35g and -49g, within the CRP site, prevent binding (Figure 3c, lanes 7-8). To determine the impact of CRP on P*murQP* activity we first used *in vitro* transcription assays (Figure 3d). Addition of CRP to reactions resulted in production of an RNA from P*murQP*. We observed similar CRP dependence *in vivo* using β-galactosidase assays (Figure 3e, compare wild type promoter activity with and without CRP). Furthermore, in wild type cells, the -35g and -49g mutations reduced promotor activity whilst the Δ183 and Δ211 truncations did not (Figure 3e). We note that the Δ211 derivative is much more active than the starting promoter DNA sequence, but transcription remains totally dependent on CRP. Most likely, the truncation removes a repressive DNA element upstream of the core promoter.
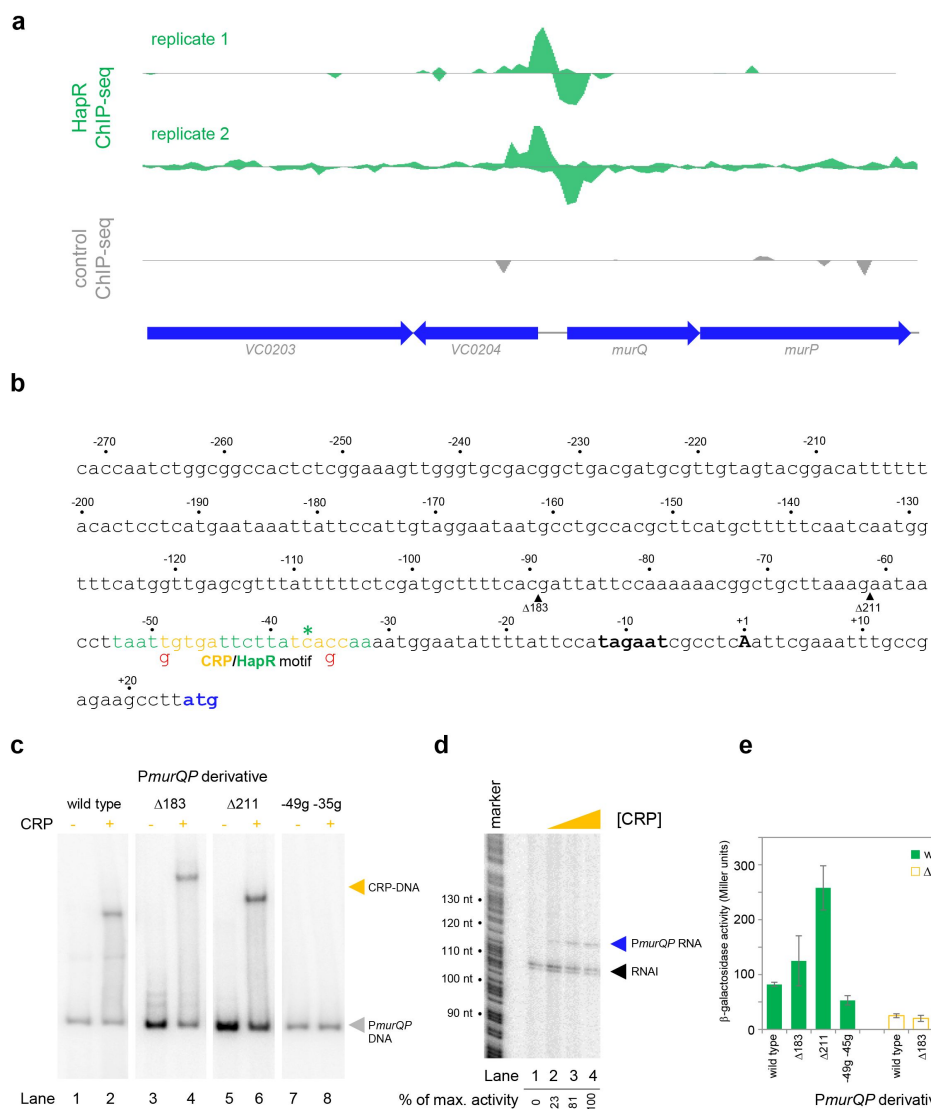
c. Binding of CRP to the *murQP* regulatory region and derivatives. Electrophoretic mobility shift assays showing migration of the *murQP* regulatory region, or indicated derivatives, with or without 0.1 μM CRP. The DNA fragment used is shown above each pair of lanes and correspond to the truncations or point mutations indicated in panel b.

d. The *murQP* promoter is activated by CRP *in vitro*. The gel image shows the result of an *in vitro* transcription assay. The DNA template was plasmid pSR carrying the *murQP* regulatory region. Experiments were done with 0.4 μM RNA polymerase with or without 0.125, 0.25, or 0.5 μM CRP. The RNAI transcript is plasmid-derived and acts as an internal control.

e. The *murQP* promoter is activated by CRP *in vivo*. The bar chart shows results of β-galactosidase activity assays. Cell lysates were obtained from wild type *V. cholerae* E7946 (solid green) or the Δ*crp* derivative, transformed with pRW50T derivatives containing the indicated promoter derivatives fused to *lacZ*. Standard deviation is shown for three independent biological replicates. Cells were grown in LB medium.

HapR and CRP bind a shared DNA site at the murQP promoter

At P*murQP*, the DNA site for CRP is completely embedded within the predicted HapR binding sequence (Figure 3b). To better understand this unusual configuration, we used DNAseI footprinting. The results are shown in Figure 4a. Lane 1 shows the pattern of DNAseI digestion in the absence of bound protein. In the presence of CRP (lanes 2-4) a footprint was observed between positions -29 and -59 bp relative to the *murQP* TSS. As is usual for CRP, and a consequence of DNA bending, the footprint comprised protection from, and hypersensitivity to, DNAse I attack. Three distinct sites of DNAseI hypersensitivity are marked by orange arrows alongside lane 4 in Figure 4a. The pattern of DNAse I digestion in the presence of HapR is shown in lanes 5-8. The footprint due to HapR binding exactly overlaps the region bound by CRP and results in complete protection of the DNA from digestion between positions -29 and -58 (green bar adjacent to lane 8). We also observed changes in the relative intensity of bands upstream of the HapR site between promoter positions -60 and -80. We speculate that this may result from changes in DNA conformation. Importantly, there was one further subtle difference between HapR and CRP induced banding patterns. Namely, in the presence of HapR, a band was observed at position -58 (see green triangle adjacent to lane 8). With CRP, a band was instead observed at position -59 (compare lanes 2-4 with 5-8). In a final set of assays, we examined addition of CRP and HapR in unison. We reasoned that 3 outcomes were possible. First, one of the two protein factors could outcompete the other. This should result in a DNAse I digestion pattern identical to either the individual CRP or HapR footprint. Second, some DNA fragments in the reaction could be bound by CRP and others by HapR. In this case, a mixed DNAse I digestion pattern, containing all features of the individual footprints due to CRP and HapR, should occur. Third, CRP and HapR could bind simultaneously. This might generate a DNAse I digestion pattern with similarities to the CRP and HapR footprints. However, accessibility of the nucleic acid to DNAse I would likely be altered in some way, with unpredictable outcomes. The result of the experiment was analysed in lanes 9-12. The binding pattern matched only some aspects of the individual footprints for CRP and HapR. Hence, we observed 2 of the 3 DNAse I hypersensitivity sites due to CRP binding. Changes in the banding pattern upstream of the binding sequence, due to HapR, were also detected. We did not observe the band at position -58 detected with HapR alone. Rather, we observed a band at position -59. An additional band at position -26 (black triangle adjacent to lane 12) was unique to these reactions. We conclude that HapR and CRP recognise the same section of the *murQP* regulatory region and may bind in unison.
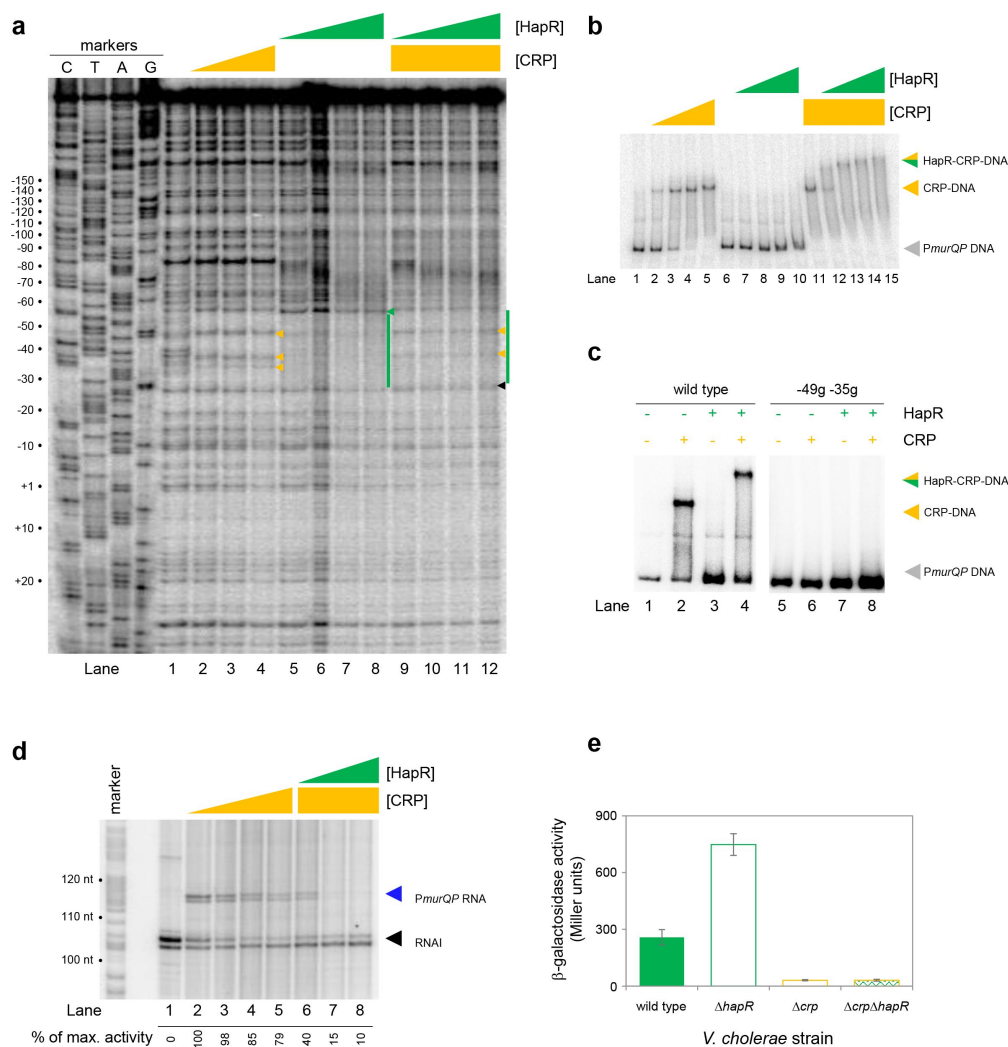
Figure 4:

HapR and CRP co-operatively bind the same section of *murQP* regulatory DNA.

a. Binding locations of HapR and CRP upstream of *murQP*. The gel shows the result of DNase I footprinting experiment. The gel is calibrated with Sanger sequencing reactions. The pattern of DNase I cleavage in the absence of any proteins is in lane 1. Protection of DNA from DNase I cleavage in the presence of 0.11, 0.23 or 0.45 µM CRP is shown in lanes 2-4. Sites of DNAse I hypersensitivity due to CRP binding are indicated by orange triangles. Protection from DNase I cleavage in the presence of 0.5, 1.0, 2.0 or 3.0 µM HapR is shown in lanes 5-8. Protection from DNase I cleavage, dependent on HapR, is shown by a green bar. A DNAse I hypersensitive band, unique to reactions with HapR, is shown by a green triangle. In the presence of 0.45 µM CRP, increasing concentrations of HapR result in a different DNAse I cleavage pattern, including the appearance of a different site of hypersensitivity (black triangle).

b. Binding of HapR and CRP upstream of *murQP* is co-operative. Electrophoretic mobility shift assays showing migration of the *murQP* regulatory region with different combinations of CRP (0.025, 0.05, 0.1 or 0.2 µM) and HapR (0.5, 1.0, 2.0, 3.0 or 4.0 µM). For incubations with both factors, the same range of HapR concentrations was used with 0.2 µM CRP.

c. Co-operative binding of CRP requires the shared HapR and CRP binding site. Results of an electrophoretic mobility shift assay, using the wild type *murQP* regulatory region or a derivative with two point mutations in the shared recognition sequence, for HapR (4.0 µM) and CRP (0.1 µM). Positions of mutations are shown in Figure 3b.

d. HapR blocks CRP mediated activation of the *murQP* promoter *in vitro*. The gel image shows the result of an *in vitro* transcription assay. The DNA template was plasmid pSR carrying the *murQP* regulatory region. Experiments were done with 0.4 µM RNA polymerase, with or without 0.05, 0.1, 0.2 or 0.5 µM CRP 0.5, 1.0, 2.0 or 3.0 µM HapR, as indicated. The RNAI transcript is plasmid-derived and acts as an internal control.

e. HapR represses CRP mediated activation of the *murQP* promoter *in vivo*. β-galactosidase activity was measured in cell lysates taken from *Vibrio cholerae* E7946 (solid green bars), Δ*hapR* derivative (open green bars), Δ*crp* variant (open

orange bars), or cells lacking both factors (orange outline with green patterned fill). Standard deviation is shown for three independent biological replicates. Cells were grown in LB medium.

HapR and CRP bind the murQP promoter co-operatively

Fragments of the *murQP* regulatory DNA, simultaneously bound by CRP and HapR, are expected to have distinct migratory properties during electrophoresis. Thus, we compared binding of CRP and/or HapR using EMSAs. The results are shown in Figure 4b. As expected, addition of CRP to reactions caused a distinct shift in electrophoretic mobility (lanes 1-5). Comparatively, at the concentration used, HapR bound the DNA fragment poorly; we observed only smearing of the free DNA at the highest HapR concentration tested (lanes 6-10). The binding pattern due to HapR was dramatically different if DNA was pre-bound with CRP (lanes 11-15). In this scenario, even low concentrations of added HapR were sufficient to generate a super-shifted nucleoprotein complex (lanes 11-15). These data are consistent with HapR having a higher affinity for CRP-P*murQP* than P*murQP* alone. Hence, HapR and CRP bind the *murQP* regulatory region co-operatively. A mundane explanation is that increased molecular crowding, upon CRP addition, increases the effective concentration of HapR. To exclude this possibility, we did two further sets of EMSA experiments. In the first set of assays, CRP was added at a lower concentration. Thus, some DNA remained unbound (Figure 4c, lanes 1 and 2). Hence, when added to such reactions, HapR could bind either the free DNA or the CRP-DNA complex. Consistent with HapR preferentially binding the latter, all of the CRP-DNA complex was super shifted upon HapR addition. Conversely, the free DNA remained unbound (compare lanes 2 and 4). In equivalent experiments, with point mutations -49g and -35g in the CRP site, neither CRP or HapR were able to bind the DNA (lanes 5-8). In a second set of tests, we used the *hapR* regulatory DNA that binds HapR but not CRP. If CRP addition increased the effective concentration of HapR, this should result in much tighter HapR binding to the *hapR* promoter. However, this was not the case (Figure S2). Taken together, our data are consistent with CRP and HapR co-operatively binding the same DNA locus at the *murQP* promoter region.

HapR represses CRP dependent transcription from the murQP promoter in vivo and in vitro

Recall that, in the absence of CRP, P*murQP* is inactive *in vitro* (Figures 2b and 3d). Furthermore, the promoter is subject to repression by HapR *in vivo* (Figure 2a). An explanation consistent with both observations is that HapR directly counteracts CRP mediated activation. To test this, we used *in vitro* transcription assays (Figure 4d). As expected, addition of CRP activated *murQP* transcription (lanes 1-4) and this was blocked by addition of HapR (lanes 5-8). We also repeated our prior *lacZ* fusion experiments, using the Δ211 P*murQP* derivative, and *V. cholerae* E7946 lacking *crp* and/or *hapR*. The result is shown in Figure 4e. Deletion of *hapR* caused increased transcription from P*murQP* only when CRP was present. Hence, HapR also represses CRP dependent *murQP* transcription *in vivo*.

Binding sites for CRP and HapR overlap in a specific configuration genome-wide

Both CRP and HapR bind the same DNA region upstream of *murPQ*. This suggests similar nucleic acid sequences are recognised by each factor. Figure 5a shows an alignment of DNA logos, derived from CRP[9] (top) and HapR (bottom) ChIP-seq targets. The two motifs have features in common that align best when the logo centres are offset by 1 base pair. This is

consistent with the arrangement of binding sites upstream of *murPQ* (Figure 3b). To understand the importance of this configuration we first took a bioinformatic approach. The DNA sequences logos shown in Figure 5a were used to create position weight matrices (PWMs) describing either the CRP or HapR binding site. We then searched the *V. cholerae* genome, using each PWM, and calculated the distance between identified CRP and HapR sites. The data for all sites within 100 bp of each other is shown in Figure 5b (top panel). In all cases, the CRP and HapR targets were offset by 1 bp. We then repeated the analysis after randomising the *V. cholerae* genome sequence (bottom panel). The number of overlapping targets was reduced 7-fold. An equivalent analysis of the *V. harveyi* genome produced similar results (Figure S3). Hence, sites for CRP and HapR have a propensity to coincide in a specific configuration. That such sites are found more frequently in native genome sequences, compared to those first randomised, suggests selection during genome evolution. We next sought to understand how this arrangement might permit simultaneous and co-operative binding of CRP and HapR.

Figure 5:

HapR contacts Activation Region 3 of CRP.

a. Binding sites for CRP and HapR are optimally aligned when offset by one base pair. The panel shows DNA sequences logos generated by aligning binding sites identified by ChIP-seq analysis for CRP (top) and HapR (bottom). The centre of each motif is indicated by a dashed line.

b. Global overlap of CRP and HapR binding sites. A position weight matrix (PWM), corresponding to each DNA sequence logo shown in panel a, was created. The PWMs were used to search the *V. cholerae* genome sequence using FIMO. Distances between the identified CRP and HapR sites were calculated. Proximal sites were always overlapping and offset by one base pair (top panel). Overlap was greatly reduced when the analysis was applied to a randomised version of the same genome sequence (bottom panel).

c. Model of the DNA-CRP-HapR complex. The model was generated using PDB submissions 6pb6 (*E. coli* CRP in complex with a class II CRP dependent promoter) and 1jt0 (*S. aureus* QacR bound to its DNA target). Note that QacR is closely related to *V. cholerae* HapR. The structures were aligned so that the CRP and HapR binding centres were offset by one base pair. Residue E55 of CRP (blue) is within Activating Region 3 of CRP that can interact with the RNA polymerase sigma subunit at class II promoters. HapR residue R123 (red) participates in HapR dimerisation and is proximal to E55 of CRP.

d. Side chain E55 of CRP is required for stability of the DNA-CRP-HapR complex. Electrophoretic mobility shift assays showing migration of the *murQP* regulatory region with different combinations of CRP or CRP^{E55A} (0.15, 0.3 or 0.6 μM) and HapR (0.083, 0.125, 0.166 0.208 or 0.25 μM).

e. HapR cannot repress transcription activated by CRP^{E55A}. Result of an *in vitro* transcription assay. The DNA template was plasmid pSR carrying the *murQP* regulatory region. Experiments were done with 0.4 μM RNA polymerase, with or without 0.05, 0.1, 0.2 or 0.5 μM CRP or CRP^{E55A} and 0.5, 1.0, 2.0 or 3.0 μM HapR, in the presence of 0.2 μM CRP, as indicated. The RNAI transcript is plasmid-derived and acts as an internal control.
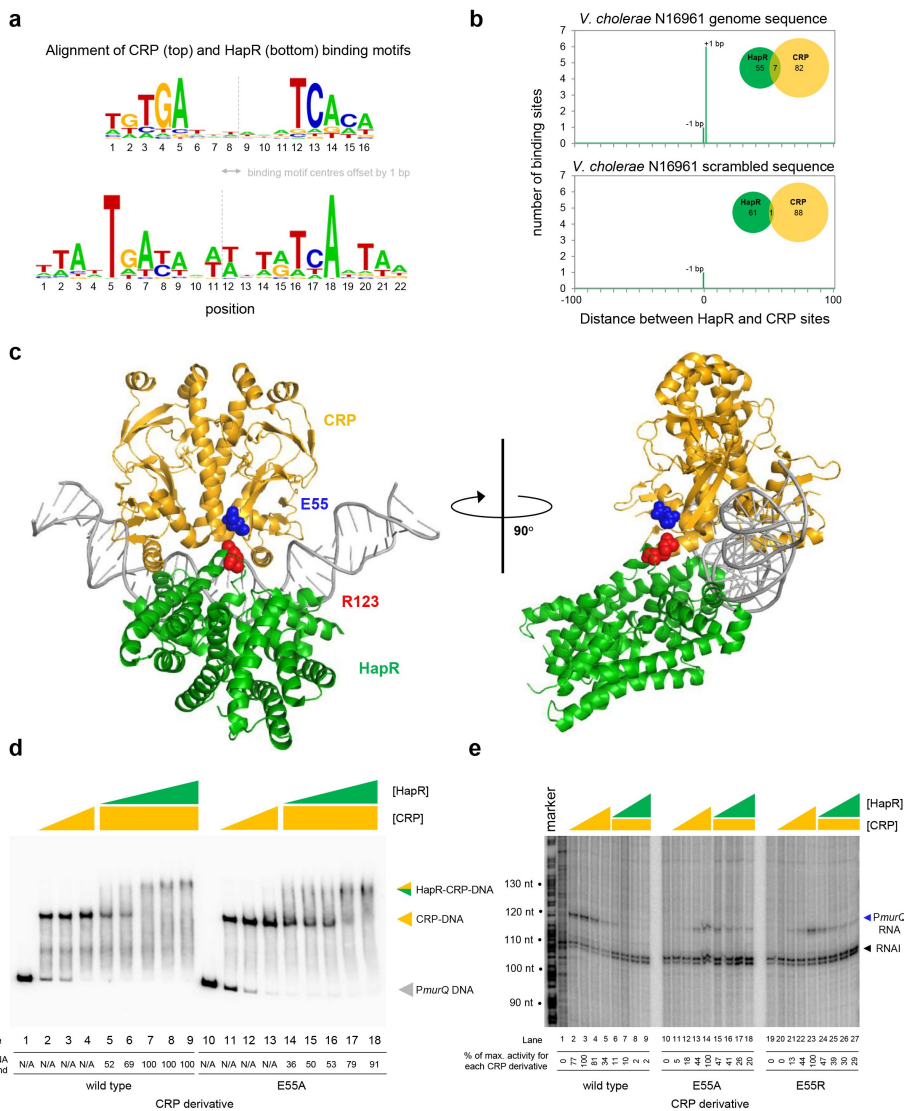
A structural model of the DNA-CRP-HapR ternary complex

To understand organisation of the DNA-CRP-HapR ternary complex we used structural modelling. The *V. cholerae* CRP protein is 96 % identical to the equivalent factor in *Escherichia coli*. Similarly, the *Staphylococcus aureus* factor QacR is 50 % similar to *V. cholerae* HapR. Previously, structural biology tools were used to investigate *E. coli* CRP, and *S. aureus* QacR, bound with their cognate DNA targets. We used this information to build a model for the DNA-CRP-HapR ternary complex. Importantly, we ensured that the CRP and HapR binding centres were offset by 1 bp. When aligned in this way, CRP and HapR recognise the same section of DNA via different surfaces of the double helix. We examined the model in the context of our DNAse I footprinting data. Recall that CRP binding upstream of *murPQ* induces three sites of DNAse I hypersensitivity (Figure 4a). These correspond to positions -47, -38 and -34 with respect to the *murQP* TSS. Figure S4 shows these positions highlighted in the context of our model. In the presence of CRP alone, all sites are surface exposed but position -34 is partially occluded by CRP (Figure S4a). This likely explains why positions -47 and -38 are more readily cleaved by DNAse I (Figure 4a). With both CRP and HapR, position -34 was completely protected from DNAse I attack (Figure 4a). Consistent with the footprinting data, our model indicates that position -34 is almost completely hidden upon binding of HapR (Figure S4b). Conversely, access to positions -47 and -38 is not altered (Compare Figures S4a and S4b).

Co-operative binding with HapR requires CRP residue E55

Co-operative DNA binding by transcription factors can result from their direct interaction[32]–[34]. In our model, a negatively charged surface of CRP (including residue E55) is in close proximity to positively charged HapR residue R123 (Figure 5c). In initial experiments, we mutated both protein surfaces to remove the charged side chain, or replace the residue with an oppositely charged amino acid. We then investigated consequences for HapR and CRP binding individually at P*murQP* using EMSAs (Figure S5). Whilst the CRP derivatives were able to bind the *murQP* regulatory region normally, HapR variants were completely defective. This is likely because R123 sits at the HapR dimerisation interface. Hence, we focused on understanding the contribution of CRP sidechain E55 to co-operative DNA binding by HapR and CRP using EMSAs. The results are shown in Figure 5d. Both wild type CRP, and CRP^{E55A}, were able to bind the *murQP* regulatory region similarly (lanes 1-4 and 10-13). As expected, HapR bound tightly to the wild type CRP:DNA complex (lanes 5-9). Conversely, HapR had a lower affinity for DNA in complex with CRP^{E55A} (lanes 14-18). This suggests that the E55A mutation in CRP destabilises the interaction with HapR.

Repression of PmurQP by HapR requires CRP residue E55

Residue E55 locates to a negatively charged surface of CRP called Activating Region 3 (AR3). This determinant aids recruitment of RNA polymerase when CRP binds close to the promoter -35 element[35]. Hence, AR3 is likely to be important for activation of P*murQP* (Figure 3b). We inferred that CRP lacking E55 should activate P*murQP* less efficiently but be less sensitive to negative effects of HapR. To test these predictions, we used *in vitro* transcription assays. The results for CRP, CRP^{E55A} and CRP^{E55R} are shown in Figure 5e. All CRP derivatives were able to activate transcription from P*murQP*. However, consistent with an important role for AR3, the ability of the CRP^{E55A} and CRP^{E55R} to activate transcription was impaired (compare lanes 1-5, 10-14 and 19-23). Crucially, whilst HapR reduced transcription dependent on wild type CRP by 50-fold (compare lane 4 with lanes 6-9) only a 2-fold effect of HapR was observed with CRP^{E55A} (compare lane 13 with lanes 15-18). In the presence of CRP^{E55R}, HapR was even less effective (compare lane 22 with lanes 24-27).

High cell density locked V. cholerae are defective for growth on MurNAc

Phosphorylated LuxO activates expression of the Qrr sRNAs that inhibit *hapR* expression at low cell density (Figure 1a). Consequently, deletion of *luxO* causes constitutive expression of HapR. Thus, Δ*luxO V. cholerae* are "locked" in a high cell density state[29]. Our model predicts that such strains will be defective for growth using MurNAc as the sole carbon source, as this requires expression of *murQP* that is repressed by HapR. Furthermore, any such defect should be relieved upon deletion of *hapR*. To test this, we constructed strains lacking different combinations of *luxO* and *hapR*. We also tested a *V. cholerae* derivative lacking *murP*[36]. Figure 6a illustrates growth in M9 minimal media, supplemented with MurNAc or glucose, and in Luria Broth. As expected, cells lacking *murP* could not grow when MurNAc was the only carbon source but were not defective in other conditions (compare grey data points in each panel). Cells lacking *hapR*, alone or in combination with *luxO*, had a similar growth defect in all conditions. Strikingly, the *luxO* mutant (high cell density locked), exhibited a growth defect only when MurNAc was the sole carbon source (compare red data points). Specifically, these cells exhibited an extended lag phase in MurNAc. This extended lag phase was not apparent when both *luxO* and *hapR* were deleted, consistent with the effect of *luxO* being mediated by HapR-dependent repression of *murQP*.
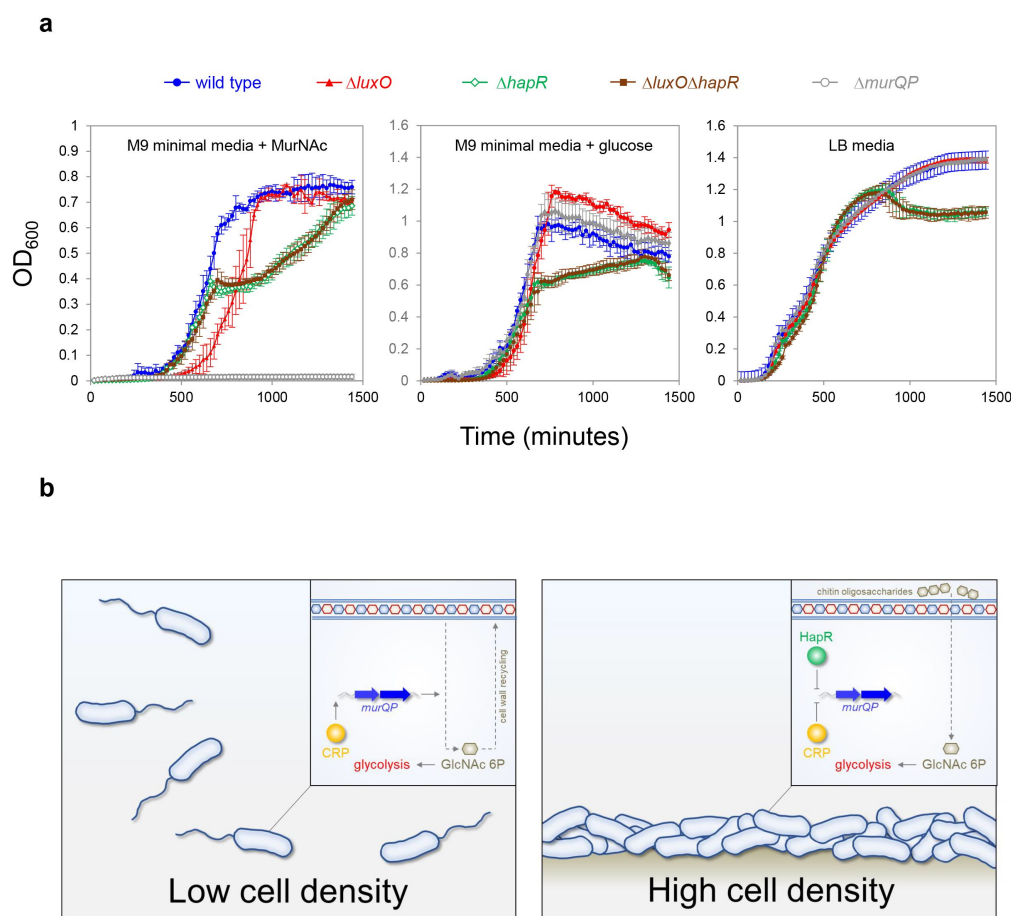
Figure 6:

Control of *murQP* expression by CRP and HapR at low and high cell density.

a. *V. cholerae* locked at high cell density are defective for growth using MurNAc as the sole carbon source. Each panel illustrates the optical density of *V. cholerae* cultures at different timepoints after inoculation. Cells lacking *luxO*, but not *luxO* and *hapR*, mimic the high cell density state. Error bars show standard deviation from three separate experimental replicates.

b. Model for coordination of MurNAc catabolism by CRP and HapR. In low *V. cholerae* population density conditions (left panel) cell division necessitates cell wall turnover. Expression of MurQP facilitates cell wall recycling and conversion of MurNAc to GlcNAc 6P for glycolysis (insert). At high cell density conditions (right panel) *V. cholerae* form biofilms on chitinous surfaces. Reduced cell division, and the availability of chitin derived GlcNAc 6P, reduces the need for MurQP.

Co-operative interactions between HapR and CRP are commonplace

In a final set of experiments, we turned our attention to other sites shared by CRP and HapR (Table 1 and prior work[9]). We selected 5 such targets and examined binding of CRP and HapR using EMSAs. At 1 target, adjacent to *VCA0218*, binding was not co-operative and free DNA remained when both proteins were present (Figure S6). For 4 of the targets, we detected co-operative binding of CRP and HapR, reminiscent of our experiments with P*murQP* DNA (Figure 4). At these loci (adjacent to *VC0102, VC1851, VCA0663* and *VCA0691*) either HapR or CRP bound poorly to DNA in the absence of the other protein. However, when both factors were added together, all DNA shifted into a distinct low mobility complex. We conclude that co-operative binding of HapR and CRP to shared targets is common.

Discussion

Previously, two studies have mapped DNA binding by HapR homologs in *Vibrio* species. For *V. harveyi*, van Kessel and co-workers used ChIP-seq to identify 105 LuxR binding targets[37]. At 77 of these sites, LuxR repressed transcription. Using ChIP-seq and global DNAse I footprinting, Zhang *et al.* found 76 LuxR bound regions in *Vibrio alginolyticus*[38]. Regulatory effects were evident for 37 targeted genes, with 22 cases of LuxR mediated repression. In the present study, we identified 32 HapR bound sections of the *V. cholerae* genome. Consistent with prior work, repression of target genes was the most common regulatory outcome. Furthermore, the DNA binding consensus derived here for HapR is almost identical to motifs for LuxR binding in *V. harveyi* and *V. alginolyticus*. Contrastingly, Tsou and colleagues used bioinformatic tools to predict HapR binding in *V. cholerae*[28]. Two different HapR binding motifs were proposed. Both partially match the HapR target sequence proposed here. Most likely, the analysis of Tsou *et al.* was hampered by a paucity of targets from which a full consensus could be derived. We note that our list of 32 HapR targets does not include all known targets. However, on inspection, whilst insufficient to pass our stringent selection criteria, weaker signals for HapR are evident at many such locations (Figure S7). In particular, we note evidence for binding of HapR upstream of *hapA*, which has previously been only inferred (Figure S7b).

Recognition of shared DNA targets provides a simple mechanism for integration of quorum sensing signals, relayed by HapR, and cAMP fluctuations, communicated by CRP. In the example presented here, HapR acts to prevent transcription activation by co-binding the same DNA target with CRP (Figure 4). Hence, at P*murQP*, the function of CRP switches from that of an activator to a co-repressor with HapR (Figure 6b). This regulatory strategy is a logical consequence of *V. cholerae* forming biofilms on chitinous surfaces. At low cell density, rapidly dividing cells must continually remodel their cell wall. In these conditions, HapR is not expressed. Thus, MurQ and MurP are produced and can convert cell wall derived MurNAc to GlcNAc-6P. Conversely, in high cell density scenarios, usually involving adherence to chitin, cells divide infrequently, and remodelling of the cell wall is not required. In addition, GlcNAc-6P can be derived readily from chitin oligosaccharides. Hence, cells locked in the high cell density state are defective for growth when supplied with MurNAc as the sole carbon source (Figure 6a). We suggest that HapR and CRP are likely to coordinate the expression of other metabolic enzymes in a similar way. Interestingly, AphA, another quorum sensing responsive regulator, also acts alongside CRP at many *V. cholerae* promoters[39]. Indeed, AphA and CRP binding sites can overlap but this results in competition between the factors[39]. Together with results presented here, these

observations highlight close integration of quorum sensing with gene control by cAMP in *V. cholerae*.

Materials and methods

Strains, plasmids and oligonucleotides

Strains, plasmids and oligonucleotides used in this study are listed in Table S1. All *V. cholerae* strains are derivatives of E7946[40]. Chromosomal deletions were made using the pKAS32 suicide plasmid for allelic exchange[41],[42] or via splicing-by-overlap-extension PCR and chitin-induced natural transformation[43]. The *E. coli* strain JCB387 was used for routine cloning[44]. Plasmids were transferred into *V. cholerae* by either conjugation or transformation as described previously[9],[39].

ChIP-seq and bioinformatics

Chromatin immunoprecipitation was done as in prior work[39] using strain E7946, carrying plasmid pAMCF-*luxO* or pAMNF-*hapR*. In both cases, control experiments were done using the equivalent plasmid with no gene insert. Note that both plasmids drive low level constitutive expression of 3xFLAG transcription factor derivatives[45]. Lysates were prepared from mid-log phase cultures, incubated with shaking at 37 °C. Following sonication, the protein-DNA complexes were immunoprecipitated with an anti-FLAG antibody (Sigma) and Protein A sepharose beads. Immunoprecipitated DNA was blunt-ended, A-tailed, and ligated to barcoded adaptors before elution and de-crosslinking. ChIP-seq libraries were then amplified by PCR and purified. Library quality was assessed using an Agilent Tapestation 4200 instrument and quantity determined by qPCR using an NEBnext library quantification kit (NEB). Libraries were sequenced as described previously[45] and reads are available from ArrayExpress using accession code E-MTAB-11906. Single-end reads, from two independent ChIP-seq experiments for each strain, were mapped to the reference *V. cholerae* N16961 genome (chromosome I: NC_002505.1 and chromosome II: NC_002506.1) with Bowtie 2[46]. The read depth at each position of the genome was determined for each BAM file using multibamsummary. Each binding profile was then normalised to an average genome-wide read depth of 1 read per base. Following normalisation, the average read depth per base for each pair of replicates was calculated. The resulting files were used to generate the circular plots in Figure 1 using DNAplotter[47]. For peak selection, the files were viewed as graphs using the Artemis genome browser[48]. After visually identifying an appropriate cut-off, peaks were selected using the "create features from graph" tool. For HapR, the window size, minimum feature size, and cut-off value were 100, 100 and 10 respectively. For LuxO, the equivalent values were 100, 100 and 4. The mid-point of features selected in this way was set as the peak centre. In each case, 300 bp of sequence from the peak centre was selected and the combined set of such sequences for each factor were analysed using MEME to generate DNA sequence logos[49].

β-galactosidase assays

Promoter DNA was fused to *lacZ* in plasmid pRW50T that can be transferred from *E. coli* to *V. cholerae* by conjugation[9]. Assays of β-galactosidase activity were done according to the Miller method[50]. Bacterial cultures were grown at 37 °C with shaking in LB broth, supplemented with appropriate antibiotics, to mid-log phase. Values shown are the mean of three independent experiments and error bars show the standard deviation.

Proteins

We purified *V. cholerae* CRP and RNA polymerase as described previously[9],[39]. To generate HapR, *E. coli* T7 Express cells were transformed with plasmid pHis-tev-HapR, or derivatives, which encodes HapR with a His$_6$ tag and intervening site for the tobacco etch virus protease protease. Transformants were cultured in 40 ml LB overnight, then subcultured in 1 L of LB, with shaking at 37 ºC. When subcultures reached midlog phase they were supplemented with 400 mM IPTG for 3 hours. Cells were then collected by centrifugation, resuspended in 40 ml of buffer 1 (40 ml 25 mM Tris-HCl pH 7.5, 1 mM EDTA and 1 M NaCl) and lysed by sonication. Inclusion bodies, recovered by centrifugation, were resuspended with 40 ml of buffer 2 (25 mM Tris-HCl pH 8.5 and 4 M urea) before the remaining solid material was again recovered and then solubilised using 40 ml of buffer 3 (25 mM Tris-HCl pH 8.5 and 6 M guanidine hydrochloride). Cleared supernatant was applied to a HisTrap HP column (GE healthcare) equilibrated with buffer A (25 mM Tris-HCl pH 8.5 and 1 M NaCl). To elute His$_6$-HapR, a gradient of buffer B (25 mM Tris-HCl pH 8.5, 1 M NaCl and 1 M imidazole) was used. Fractions containing His$_6$-HapR were pooled and the protein was transferred into buffer X (50 mM HEPES, 1 M NaCl, 1 mM DTT, 5 mM EDTA and 0.1 mM Triton X-100) by dialysis. Finally, we used Vivaspin ultrafiltration columns to reduce sample volume. The concentration of His$_6$-HapR was then determined.

in vitro *transcription assays*

Experiments were done using our prior approach[39]. Plasmid templates were isolated from *E. coli* using Qiagen Maxiprep kits. Each *in vitro* transcription assay contained 16 µg/ml DNA template in 40 mM Tris pH 7.9, 5 mM MgCl2, 500 µM DTT, 50 mM KCl, 100 µg/ml BSA, 200 µM ATP/GTP/CTP, 10 µM UTP and 5 µCi α-P32-UTP. Purified HapR and CRP were added at the indicated concentrations prior to the reaction start point. In experiments where CRP was used, the protein was incubated with cAMP 37 ºC prior to addition. Transcription was instigated by addition of RNA polymerase holoenzyme prepared in advance by incubation of the core enzyme with a 4-fold excess of σ^{70} for 15 minutes at room temperature. After 10 minutes incubation at 37 °C, reactions were stopped by the addition of an equal volume of formamide containing stop buffer. Reactions were resolved on an 8% (*w/v*) denaturing polyacrylamide gel, exposed on a Bio-Rad phosphor screen then visualised on a Bio-Rad Personal Molecular Imager. The quantify transcript levels, we measured the intensity of bands corresponding to RNAI and the RNA of interest using Quantity One software. After subtracting background lane intensity, we calculated the RNA of interest to RNAI ratio. The maximum ratio was set to 100 % activity with other ratios shown a percentage of this maximum.

Electrophoretic mobility shift assays and DNAse I footprinting

Promoter DNA fragments were excised from plasmid pSR and end-labelled with γ32-ATP using T4 PNK (NEB). EMSAs and DNase I footprints were done as previously described [39]. Full gel images are shown in Figure S8.

Structural modelling

The model of the ternary DNA-CRP-HapR complex was generated in PyMOL by aligning PDB depositions 1jt0 (QacR-DNA complex) and 6pb6 (CRP-DNA complex). Alignments were done manually and guided by the relative two-fold centres of symmetry for each complex. Each structure was positioned so that their DNA base pairs overlapped and binding centres were offset by 1 base pair. The Mutagenesis function of PyMOL was used to replace QacR

sidechain K107, equivalent to HapR R123[20], with an arginine residue. The double helix of the QacR DNA complex is hidden in the final model.

Acknowledgements

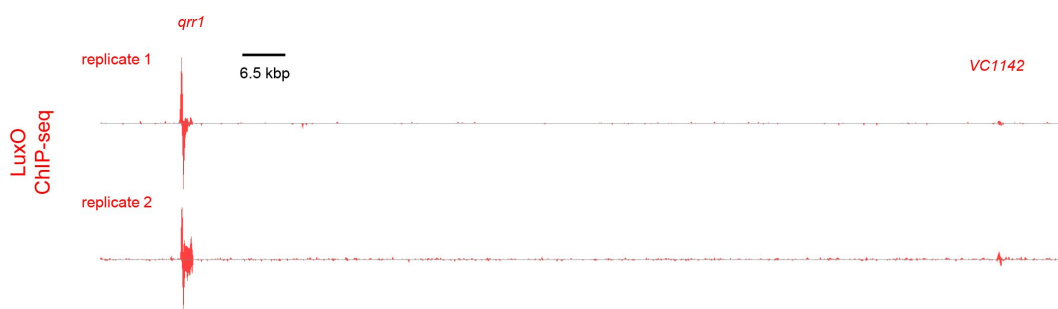# Supplementary figure legends

Figure S1:

Binding of LuxO and the *qrr1* and *VC1142* loci.

ChIP-seq coverage plots are shown for individual experimental replicates. Signals above or below the horizontal line correspond to reads mapping to the top or bottom strand respectively.
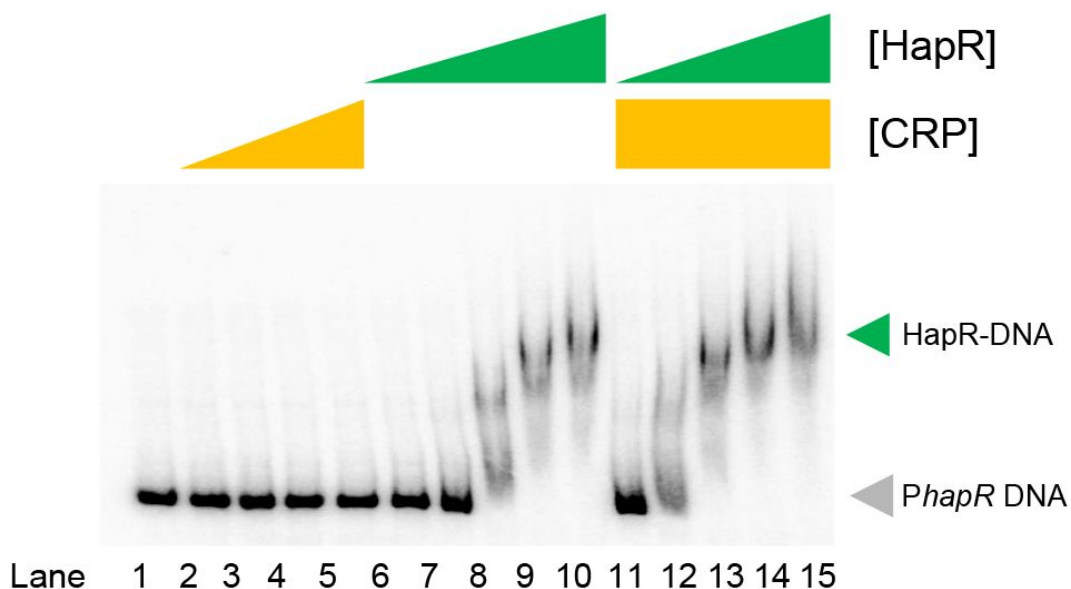
Figure S2:

Binding of HapR to the *hapR* promoter region in the presence and absence of CRP.

Electrophoretic mobility shift assay showing migration of the *hapR* regulatory region with different combinations of CRP (0.0125, 0.025, 0.05 or 0.1 µM) and HapR (0.0625, 0.125, 0.25 or 0.5 µM). For incubations with both factors, the same range of HapR concentrations was used with 0.1 µM CRP.

a

CRP

-34

-38

DNAse I hypersensitivity

-34

-47

-38

b

HapR

-38

-47

Figure S5:

Binding of CRP and HapR derivatives to P*murQP*.

The figures shows results of electrophoretic mobility shift assays with CRP and derivatives (0.1, 0.2, 0.4 or 0.8 µM) or HapR and derivatives (0.25, 0.5, 1.0, 2.0 or 4.0 µM).
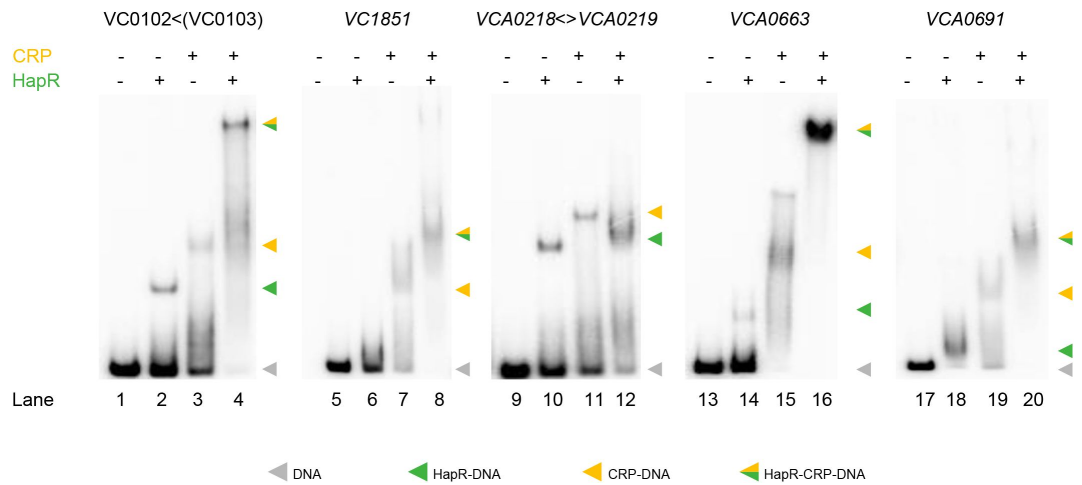
Lane: 1 2 3 4 | 5 6 7 8 | 9 10 11 12 | 13 14 15 16 | 17 18 19 20

VC0102<(VC0103) | *VC1851* | *VCA0218<>VCA0219* | *VCA0663* | *VCA0691*

CRP: - - + + | - - + + | - - + + | - - + + | - - + +
HapR: - + - + | - + - + | - + - + | - + - + | - + - +

◁ DNA   ◀ HapR-DNA   ◀ CRP-DNA   ◀ HapR-CRP-DNA

Figure S6:

Co-operative DNA binding of HapR and CRP is common.

Electrophoretic mobility shift assays showing migration of the indicated regulatory regions with different combinations of CRP (1 μM) and HapR (0.19 μM). For *VCA0691* the concentration of HapR was 0.57 μM.
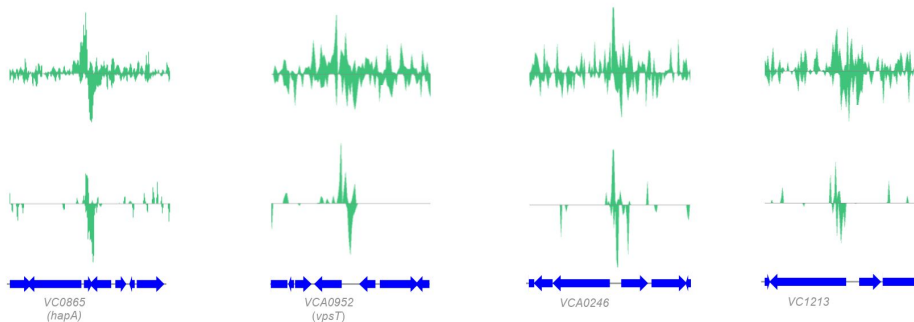
a
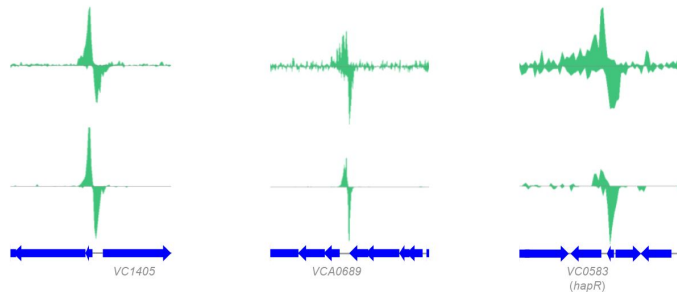
b

Figure S7:

Example HapR binding signals.

a. Binding peaks for HapR that fall above our cut-off for peak selection. The HapR ChIP-seq binding profiles are shown in green and genes are shown as blue arrows.

b. Binding peaks for HapR, at known targets, that fall below our cut-off for peak selection. Binding signals for HapR are shown at known target genes. These peaks for not selected by our analysis because the signal was too weak and/or insufficiently reproducible.
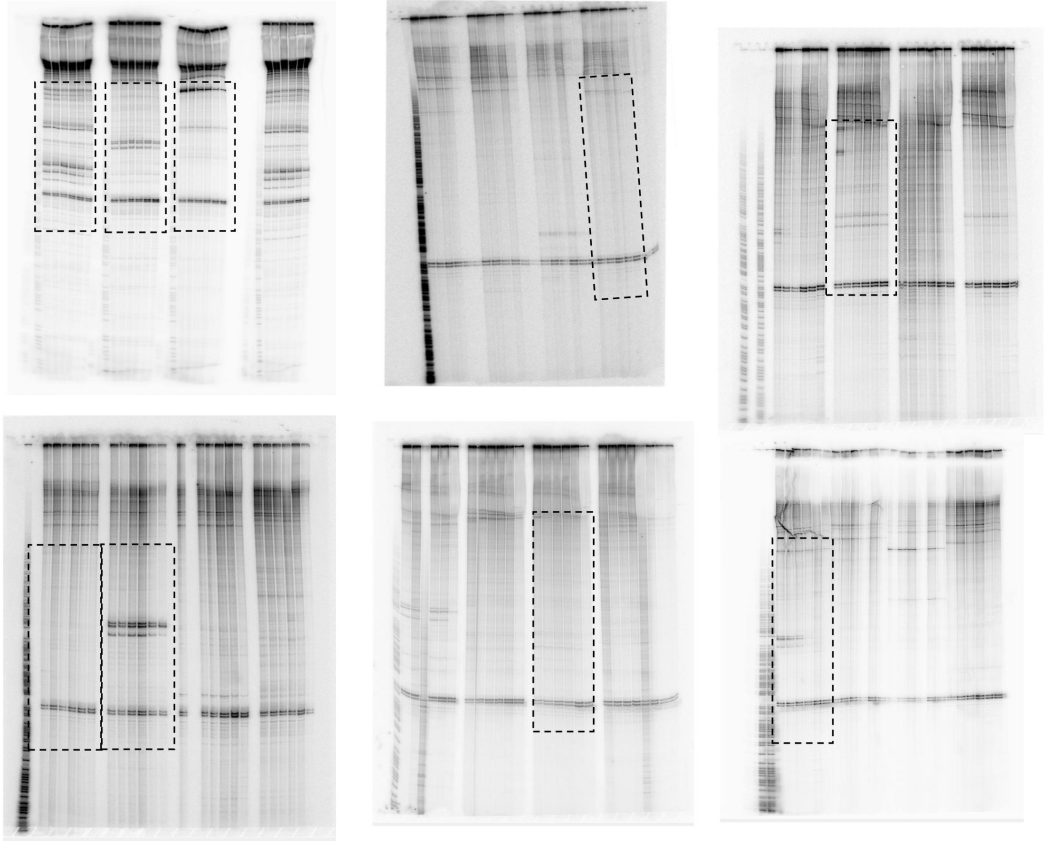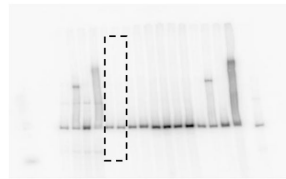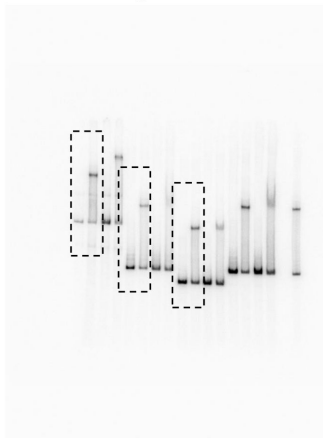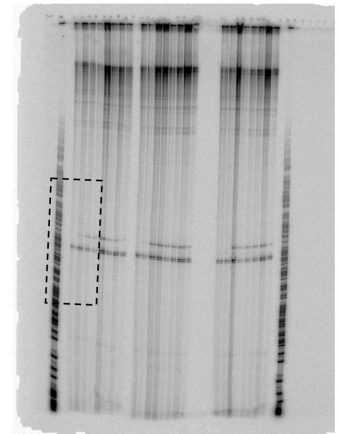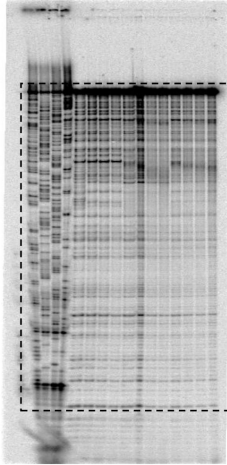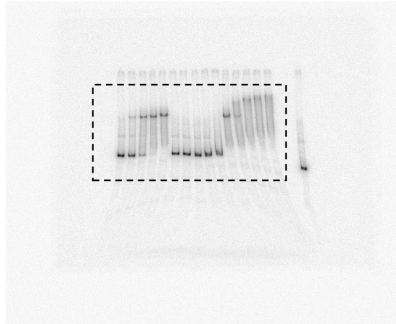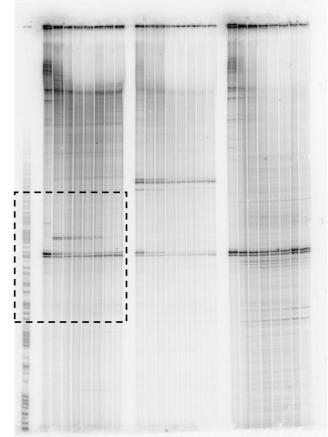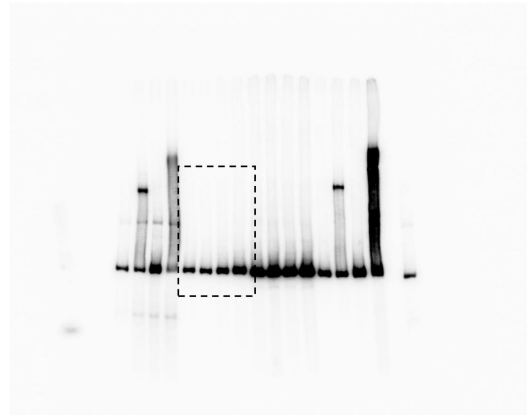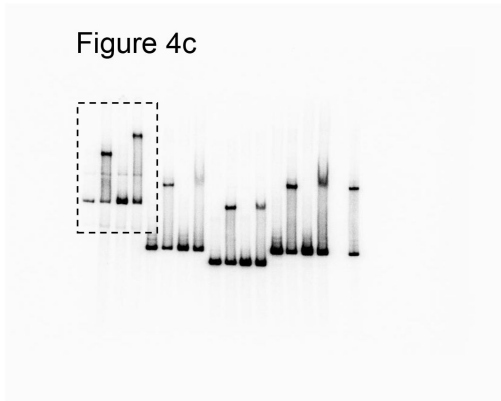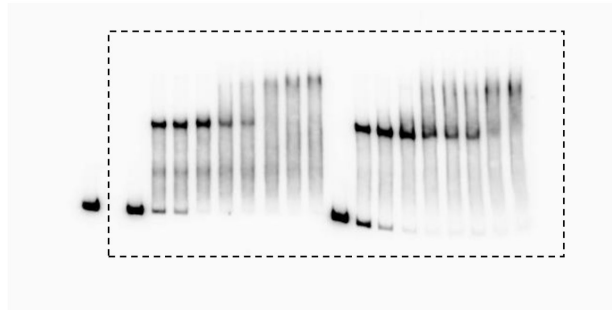
Figure 4a

Figure 4b

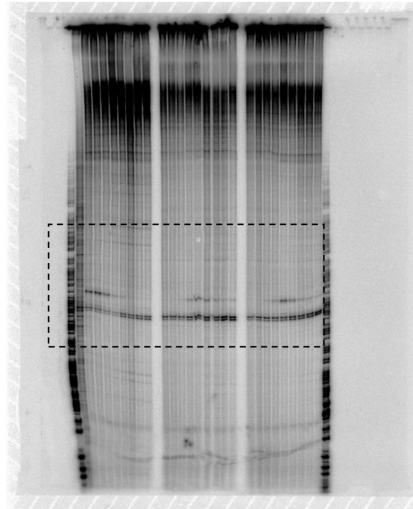Figure 4d

Figure 4c

Figure 5d

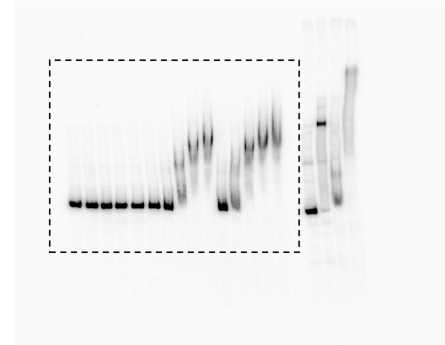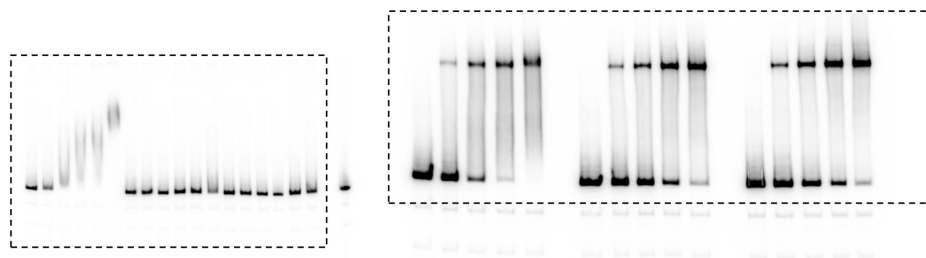Figure 5e
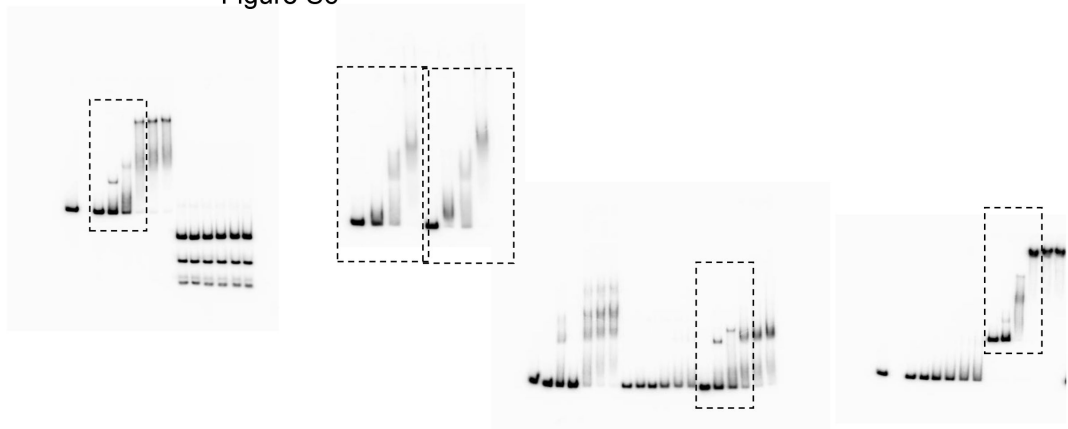

Figure S2

Figure S5

Figure S6

Figure S8:

Original gel images.

References

1. Nelson E. J. , Harris J. B. , Morris J. G. , Calderwood S. B. , Camilli A. (2009) **Cholera transmission: The host, pathogen and bacteriophage dynamic** *Nature Reviews Microbiology* **7:**693–702

2. Ali M. , Nelson A. R. , Lopez A. L. , Sack D. A. (2015) **Updated Global Burden of Cholera in Endemic Countries** *PLoS Negl. Trop. Dis* **9:**

3. Domman D. (2017) **Integrated view of Vibrio cholerae in the Americas** *Science* **358:**789–793

4. Asadgol Z. , Mohammadi H. , Kermani M. , Badirzadeh A. , Gholami M. (2019) **The effect of climate change on cholera disease: The road ahead using artificial neural network** *PLoS One* **14:**

5. Meiborn K. L. (2004) **The Vibrio cholerae chitin utilization program** *PNAS* **101:**2524–2529

6. Hung D. T. , Mekalanos J. J. (2005) **Bile acids induce cholera toxin expression in Vibrio cholerae in a ToxT-independent manner** *PNAS* **102:**3028–3033

7. Weber G. G. , Kortmann J. , Narberhaus F. , Klose K. E. (2014) **RNA thermometer controls temperature-dependent virulence factor expression in Vibrio cholerae** *PNAS* **111:**14241–14246

8. Krasteva P. V. (2010) **Vibrio cholerae vpst regulates matrix production and motility by directly sensing cyclic di-GMP** *Science* **327:**866–868

9. Manneh-Roussel J. (2018) **Camp receptor protein controls Vibrio cholerae gene expression in response to host colonization** *MBio* **9:**

10. Kamareddine L. (2018) **Activation of Vibrio cholerae quorum sensing promotes survival of an arthropod host** *Nat. Microbiol* **3:**243–252

11. Weill F.-X. (2017) **Genomic history of the seventh pandemic of cholera in Africa** *Science* **358:**785–789

12. Eickhoff M. J. , Bassler B. L. (2018) **SnapShot: Bacterial Quorum Sensing** *Cell* **174:**1328–1328

13. Mukherjee S. , Bassler B. L. (2019) **Bacterial quorum sensing in complex and dynamically changing environments** *Nature Reviews Microbiology* **17:**371–382

14. Henke J. M. , Bassler B. L. (2004) **Three parallel quorum-sensing systems regulate gene expression in Vibrio harveyi** *J. Bacteriol* **186:**6902–6914

15. Freeman J. A. , Bassler B. L. (1999) **A genetic analysis of the function of LuxO, a two-component response regulator involved in quorum sensing in Vibrio harveyi** *Mol. Microbiol* **31:**665–677

16. Freeman J. A. , Bassler B. L. (1999) **Sequence and function of LuxU: A two-component phosphorelay protein that regulates quorum sensing in Vibrio harveyi** *J. Bacteriol* **181:**899–906

17. Lenz D. H. (2004) **The small RNA chaperone Hfq and multiple small RNAs control quorum sensing in Vibrio harveyi and Vibrio cholerae** *Cell* **118:**69–82

18. Shao Y. , Bassler B. L. (2012) **Quorum-sensing non-coding small RNAs use unique pairing regions to differentially control mRNA targets** *Mol. Microbiol* **83:**599–611

19. Rutherford S. T. , Van Kessel J. C. , Shao Y. , Bassler B. L. (2011) **AphA and LuxR/HapR reciprocally control quorum sensing in vibrios** *Genes Dev* **25:**397–408

20. De Silva R. S. (2007) **Crystal structure of the Vibrio cholerae quorum-sensing regulatory protein HapR** *J. Bacteriol* **189:**5683–5691

21. Jobling M. G. , Holmes R. K. (1997) **Characterization of hapR, a positive regulator of the Vibrio cholerae HA/protease gene hap, and its identification as a functional homologue of the Vibrio harveyi luxR gene** *Mol. Microbiol* **26:**1023–1034

22. Heidelberg J. F. (2000) **DNA sequence of both chromosomes of the cholera pathogen Vibrio cholerae** *Nature* **406:**477–483

23. Nielsen A. T. (2006) **RpoS controls the Vibrio cholerae mucosal escape response** *PLoS Pathog* **2:**933–948

24. Van Kessel J. C. , Rutherford S. T. , Shao Y. , Utria A. F. , Bassler B. L. (2013) **Individual and combined roles of the master regulators apha and luxr in control of the Vibrio harveyi quorum-sensing regulon** *J. Bacteriol* **195:**436–443

25. Silva A. J. , Benitez J. A. (2004) **Transcriptional regulation of Vibrio cholerae hemagglutinin/protease by the cyclic AMP receptor protein and RpoS** *J. Bacteriol* **186:**6374–6382

26. Tu K. C. , Bassler B. L. (2007) **Multiple small RNAs act additively to integrate sensory information and control quorum sensing in Vibrio harveyi** *Genes Dev* **21:**221–233

27. Lin W. , Kovacikova G. , Skorupski K. (2005) **Requirements for Vibrio cholerae HapR binding and transcriptional repression at the hapR promoter are distinct from those at the aphA promoter** *J. Bacteriol* **187:**3013–3019

28. Tsou A. M. , Cai T. , Liu Z. , Zhu J. , Kulkarni R. V. (2009) **Regulatory targets of quorum sensing in Vibrio cholerae: Evidence for two distinct HapR-binding motifs** *Nucleic Acids Res* **37:**2747–2756

29. Waters C. M. , Lu W. , Rabinowitz J. D. , Bassler B. L. (2008) **Quorum sensing controls biofilm formation in Vibrio cholerae through modulation of cyclic Di-GMP levels and repression of vpsT** *J. Bacteriol* **190:**2527–2536

30. Papenfort K. , Förstner K. U. , Cong J. P. , Sharma C. M. , Bassler B. L. (2015) **Differential RNA-seq of Vibrio cholerae identifies the VqmR small RNA as a regulator of biofilm formation** *PNAS* **112:**

31. Savery N. J. (1998) **Transcription activation at class II CRP-dependent promoters: Identification of determinants in the C-terminal domain of the RNA polymerase α subunit** *EMBO J* **17:**3439–3447

32. Wade J. T. , Belyaeva T. A. , Hyde E. I. , Busby S. J. W. (2002) **A simple mechanism for co-dependence on two activators at an Escherichia coli promoter** *EMBO J* **20:**7160–7167

33. Kallipolitis B. H. , Nørregaard-Madsen M. , Valentin-Hansen P. (1997) **Protein-protein communication: Structural model of the repression complex formed by CytR and the global regulator CRP** *Cell* **89:**1101–1109

34. Meibom K. L. , Kallipolitis B. H. , Ebright R. H. , Valentin-Hansen P. (2000) **Identification of the subunit of cAMP receptor protein (CRP) that functionally interacts with CytR in CRP-CytR-mediated transcriptional repression** *J. Biol. Chem* **275:**11951–11956

35. Rhodius V. A. , Busby S. J. W. (2000) **Interactions between Activating Region 3 of the Escherichia coli cyclic AMP receptor protein and region 4 of the RNA polymerase σ70 subunit: Application of suppression genetics** *J. Mol. Biol* **299:**311–324

36. Hayes C. A. , Dalia T. N. , Dalia A. B. (2017) **Systematic genetic dissection of PTS in Vibrio cholerae uncovers a novel glucose transporter and a limited role for PTS during infection of a mammalian host** *Mol. Microbiol* **104:**568–579

37. van Kessel J. C. , Ulrich L. E. , Zhulin I. B. , Bassler B. L. (2013) **Analysis of activator and repressor functions reveals the requirements for transcriptional control by LuxR, the master regulator of quorum sensing in Vibrio harveyi** *MBio* **4:**

38. Zhang J. (2021) **Binding site profiles and N-terminal minor groove interactions of the master quorum-sensing regulator LuxR enable flexible control of gene activation and repression** *Nucleic Acids Res* **49:**3274–3293

39. Haycocks J. R. J. J. (2019) **The quorum sensing transcription factor AphA directly regulates natural competence in Vibrio cholerae** *PLoS Genet* **15:**

40. Levine M. M. (1982) **The pathogenicity of nonenterotoxigenic vibrio cholerae serogroup 01 biotype ei tor isolated from sewage water in brazil** *J. Infect. Dis* **145:**296–299

41. Skorupski K. , Taylor R. K. (1996) **Positive selection vectors for allelic exchange** *Gene* **169:**47–52

42. Dalia A. B. , McDonough E. K. , Camilli A. (2014) **Multiplex genome editing by natural transformation** *PNAS* **111:**8937–8942

43. Dalia A. B. (2018) **Natural cotransformation and multiplex genome editing by natural transformation (MuGENT) of vibrio cholerae** *in Methods in Molecular Biology* **1839:**53–64

44. Page L. , Griffiths L. , Cole J. A. (1990) **Different physiological roles of two independent pathways for nitrite reduction to ammonia by enteric bacteria** *Arch. Microbiol* **154:**349–354

45. Sharma P. (2017) **The multiple antibiotic resistance operon of enteric bacteria controls DNA repair and outer membrane integrity** *Nat. Commun* **8:**1444

46. Langmead B. , Salzberg S. L. (2012) **Fast gapped-read alignment with Bowtie 2** *Nat. Methods* **9:**357–359

47. Carver T. , Thomson N. , Bleasby A. , Berriman M. , Parkhill J. (2008) **DNAPlotter: circular and linear interactive genome visualization** *Bioinformatics* **25:**119–120

48. Carver T. , Harris S. R. , Berriman M. , Parkhill J. , Mcquillan J. A. (2012) **Carver, T., Harris, S. R., Berriman, M., Parkhill, J. & Mcquillan, J. A.Artemis: an integrated platform for visualization and analysis of high-throughput sequence-based experimental data. 28, 464–469 (2012).** *Artemis: an integrated platform for visualization and analysis of high-throughput sequence-based experimental data* **28:**464–469

49. Bailey T. L. (2009) **MEME Suite: Tools for motif discovery and searching** *Nucleic Acids Res* **37:**

50. Miller J. (1972) **Experiments in molecular genetics** *Experiments in molecular genetics*

Author information

1. **Lucas M. Walker**

   School of Biosciences, University of Birmingham, Edgbaston B15 2TT, UK

2. **James R.J. Haycocks**

   School of Biosciences, University of Birmingham, Edgbaston B15 2TT, UK

3. **Julia C. van Kessel**

   Department of Biology, Indiana University, Bloomington, Indiana, USA
   ORCID iD: 0000-0002-1612-2403

4. **Triana N. Dalia**

   Department of Biology, Indiana University, Bloomington, Indiana, USA

5. **Ankur B. Dalia**

   Department of Biology, Indiana University, Bloomington, Indiana, USA

6. **David C. Grainger**

   School of Biosciences, University of Birmingham, Edgbaston B15 2TT, UK

   For correspondence:

   d.grainger@bham.ac.uk
   ORCID iD: 0000-0003-3375-5154

Editors

Reviewing Editor
Arturo Casadevall
Johns Hopkins Bloomberg School of Public Health, United States of America

Senior Editor
Arturo Casadevall
Johns Hopkins Bloomberg School of Public Health, United States of America

Reviewer #1 (Public Review):

This manuscript by Walker et. al. explores the interplay between the global regulators HapR (the QS master high cell density (HDC) regulator) and CRP. Using ChIP-Seq, the authors find that at several sites, the HapR and CRP binding sites overlap. A detailed exploration of the murPQ promoter finds that CRP binding promotes HapR binding, which leads to repression of murPQ. The authors have a comprehensive set of experiments that paints a nice story providing a mechanistic explanation for converging global regulation. I did feel there are some weak points though, in particular the lack of integration of previously identified transcription start sites, the lack of replication (at least replication presented in the manuscript) for many figures, some oddities in the growth curve, and not reexamining their HapR/CRP cooperative binding model in vivo using ChIP-Seq.

Reviewer #2 (Public Review):

This manuscript by Walker et al describes an elegant study that synergizes our knowledge of virulence gene regulation of Vibrio cholerae. The work brings a new element of regulation for CRP, notably that CRP and the high density regulator HapR co-occupy the same site on the DNA but modeling predicts they occupy different faces of the DNA. The DNA binding and structural modeling work is nicely conducted and data of co-occupation are convincing. The work could benefit from doing a better job in the manuscript preparation to integrate the findings into our current state of knowledge of HapR and CRP regulated genes and to elevate the impact of the work to address how bacteria are responding to the nutritional environment. Importantly, the focus of the work is heavily based on the impact of use of GlcNAc as a carbon source when bacteria bind to chitin in the environment, but absent the impact during infection when CRP and HapR have known roles. Further, the impact on biological events controlled by HapR integration with the utilization of carbon sources (including biofilm formation) is not explored. The rigor and reproducibility of the work needs to be better conveyed.

Specific comments to address:

1. Abstract. A comment on the impact of this work should be included in the last sentence. Specifically, how the integration of CRP with QS for gene expression under specific environments impacts the lifestyle of Vc is needed. The discussion includes comments regarding the impact of CRP regulation as a sensor of carbon source and nutrition and these could be quickly summarized as part of the abstract.
2. Line 74. This paper examines the overlap of HapR with CRP, but ignores entirely AphA. HapR is repressed by Qrrs (downstream of LuxO-P) while AphA is activated by Qrrs. WithLuxO activating AphA, it has a significant sized "regulon" of genes turned

on at low density. It seems reasonable that there is a possibility of overlap also between CRP and AphA. While doing an AphA CHIP-seq is likely outside the scope of this work, some bioinformatic or simply a visual analysis of the promoters known AphA regulated genes would be interest to comment on with speculation in the discussion and/or supplement.

3. Line 100. Accordingly with the above statement, the focus here on HapR indicates that the focus is on gene expression via LuxO and HapR, at high density. Thus the sentence should read "we sought to map the binding of LuxO and HapR of V. cholerae genome at high density".

4. Line 109. The identification of minor LuxO binding site in the intergenic region between VC1142 and VC1143 raises whether there may be a previously unrecognized sRNA here. As another panel in figure S1, can you provide a map of the intergenic region showing the start codons and putative -10 to -35 sites. Is there room here for an sRNA? Is there one known from the many sRNA predictions / identifications previously done? Some additional analysis would be helpful.

5. Line 117. This sentence states that the CHIP seq analysis in this study includes previously identified HapR regulated genes, but does not reveal that many known HapR regulated genes are absent from Table 1 and thus were missed in this study. Of 24 HapR regulated investigated by Tsou et al, only 1 is found in Table 1 of this study. A few are commented in the discussion and Figure S7. It might be useful to add a Venn Diagram to Figure 1 (and list table in supplement) for results of Tsou et al, Waters et al, Lin et al, and Nielson et al and any others). A major question is whether the trend found here for genes identified by CHIP-seq in this study hold up across the entire HapR regulon. There should also be comments in the discussion on perhaps how different methods (including growth state and carbon sources of media) may have impacted the complexity of the regulon identified by the different authors and different methods.

6. The transcription data are generally well performed. In all figures, add comments to the figure legends that the experiments are representative gels from n=# (the number of replicate experiments for the gel based assays). Statements to the rigor of the work are currently missing.

7. Line 357-360. The demonstration of lack of growth on MurNAc is a nice for the impact of the work. However, more detailed comments are needed for M9 plus glucose for the uninformed reader to be reminded that growth in glucose is also impaired due to lack of cAMP in glucose replete conditions and thus minimal CRP is active. But why is this now dependent of hapR? A reminder also that in LB oligopeptides from tryptone are the main carbon source and thus CRP would be active.

8. A great final experiment to demonstrate the model would have been to show co-localization of the promoter by CRP and HapR from bacteria grown in LB media but not in LB+glucose or in M9+glycerol and M9+MurNAc but not M9+glucose. This would enhance the model by linking more directly to the carbon sources (currently only indirect via growth curves)

9. Discussion. Comments and model focus heavily on GlcNAc-6P but HapR has a regulator role also during late infection (high density). How does CRP co-operativity impact during the in vivo conditions? Does the Biphasic role of CRP play a role here (PMID: 20862321)?

Reviewer #3 (Public Review):

Bacteria sense and respond to multiple signals and cues to regulate gene expression. To define the complex network of signaling that ultimately controls transcription of many genes in cells requires an understanding of how multiple signaling systems can converge to effect gene expression and ensuing bacterial behaviors. The global transcription factor CRP

has been studied for decades as a regulator of genes in response to glucose availability. It's direct and indirect effects on gene expression have been documented in E. coli and other bacteria including pathogens including Vibrio cholerae. Likewise, the master regulator of quorum sensing (QS), HapR), is a well-studied transcription factor that directly controls many genes in Vibrio cholerae and other Vibrios in response to autoinducer molecules that accumulate at high cell density. By contrast, low cell density gene expression is governed by another regulator AphA. It has not yet been described how HapR and CRP may together work to directly control transcription and what genes are under such direct dual control.

Using both in vivo methods with gene fusions to lacZ and in vitro transcription assays, the authors proceed to identify the smaller subset of genes whose transcription is directly repressed (7) and activated (2) by HapR. Prior work from this group identified the direct CRP binding sites in the V. cholerae genome as well as promoters with overlapping binding sites for AphA and CRP, thus it appears a logical extension of these prior studies is to explore here promoters for potential integration of HapR and CRP. Inclusion of this rationale was not included in the introduction of CRP protein to the in vitro experiments.

Seven genes are found to be repressed by HapR in vivo, the promoter regions of only six are repressed in vitro with purified HapR protein alone. The authors propose and then present evidence that the seventh promoter, which controls murPQ, requires CRP to be repressed by HapR both using in vivo and vitro methods. This is a critical insight that drives the rest of the manuscripts focus.

The DNase protection assay conducted supports the emerging model that both CRP and HapR bind at the same region of the murPQ promoter, but interpret is difficult due to the poor quality of the blot. There are areas of apparent protection at positions +1 to +15 that are not discussed, and the areas highlighted are difficult to observe with the blot provided.

The model proposed at the end of the manuscript proposes physiological changes in cells that occur at transitions from the low to high cell density. Experiments in the paper that could strengthen this argument are incomplete. For example, in Fig. 4e it is unclear at what cell density the experiment is conducted. The results with the wild type strain are intermediate relative to the other strains tested. Cell density should affect the result here since HapR is produced at high density but not low density. This experiment would provide important additional insights supporting their model, by measuring activity at both cell densities and also in a ☐luxO mutant locked at the high cell density. Conducting this experiment in conditions lacking and containing glucose would also reveal whether high glucose conditions mimicking the ☐crp results.

Throughout the paper it was challenging to account for the number of genes selected, the rationale for their selection, and how they were prioritized. For example, the authors acknowledged toward the end of the Results section that in their prior work, CRP and HapR binding sites were identified (line 321-22). It is unclear whether the loci indicated in Table 1 all from this prior study. It would be useful to denote in this table the seven genes characterized in Figure 2 and to provide the locus tag for murPQ. Of the 32 loci shown in Table 1, five were selected for further study using EMSA (line 322), but no rationale is given for studying these five and not others in the table.

Since prior work identified a consensus CRP binding motif, the authors identify the DNA sequence to which HapR binds overlaps with a sequence also predicted to bind CRP. Genome analysis identified a total of seven sites where the CRP and HapR binding sites were offset by one nucleotide as see with murPQ. Lines 327-8 describe EMSA results with several of these DNA sequences but provides no data to support this statement. Are these loci in Table 1?

Using structural models, the authors predict that HapR repression requires protein-protein interactions with CRP. Electromobility shift assays (EMSA) with purified promoter DNA, CRP

and HapR (Fig 5d) and in vitro transcription using purified RNAP with these factors (Figure 5e) support this hypothesis. However, the model proports that HapR "bound tightly" and that it also had a "lower affinity" when CRP protein was used that had mutations in a putative interaction interface. These claims can be bolstered if the authors calculate the dissociation constant (Kd) value of each protein to the DNA. This provides a quantitative assessment of the binding properties of the proteins. The concentrations of each protein are not indicated in panels of the in vitro analysis, but only the geometric shapes denoting increasing protein levels. Panel 5e appears to indicate that an intermediate level of CRP was used in the presence of HapR, which presumably coincides with levels used in lane 4, but rationale is not provided. How well the levels of protein used in vitro compare to levels observed in vivo is not mentioned.

The authors are commended for seeking to connect the in vitro and vivo results obtained under lab conditions with conditions experienced by V. cholerae in niches it may occupy, such as aquatic systems. The authors briefly review the role of MurPQ in recycling of the cell wall of V. cholerae by degrading MurNAc into GlcNAc, although no references are provided (lines 146-50). Based on this physiology and results reported, the authors propose that murPQ gene expression by these two signal transduction pathways has relevance in the environment, where Vibrios, including V. cholerae, forms biofilms on exoskeleton composed of GlcNAc.

The conclusions of that work are supported by the Results presented but additional details in the text regarding the characteristics of the proteins used (Kd, concentrations) would strengthen the conclusions drawn. This work provides a roadmap for the methods and analysis required to develop the regulatory networks that converge to control gene expression in microbes. The study has the potential to inform beyond the sub-filed of Vibrios, QS and CRP regulation.